Peak Finding in Heavy Ion Physics by Wavelets

G.A. Ososkov
Laboratory of Information Technologies, JINR
A.V. Stadnik
Veksler and Baldin Laboratory of High Energies, JINR

Abstract

A new efficient algorithm on the wavelet basis is proposed for detecting resonance peaks from invariant mass spectra. Different wavelet families are used in the analysis. The algorithm was tested on both simulated and real data.

1 Introduction

The invariant mass method as very effective one is, therefore, one of the most usable tools for data analysis in relativistic heavy ion physics. However there are serious problems with extracting rare or short lived particle resonances in question from invariant mass spectra because of the presence of bulky background, which dramatically increases when the event multiplicity grows.

Two approaches are mostly used to overcome this problem: either to approximate the spectrum pedestal by some appropriate function (usually a polynomial) and then to subtract it from the spectrum or, more effective, but cumbersome, to simulate the pedestal by Monte Carlo as a combination of background particles contributing to the same event and then again to subtract it from the spectrum. An example of $\pi^+\pi^-$ invariant mass spectrum taken from our previous study [1] is depicted in fig.1. One can see almost invisible peak of K^0_S invariant mass = 0.49765 observed from STAR(RHIC, BNL) d-Au data at 200 Gev in fig.1(a). Result of its handling by subtraction of combinatorial background is shown in fig.1(b).

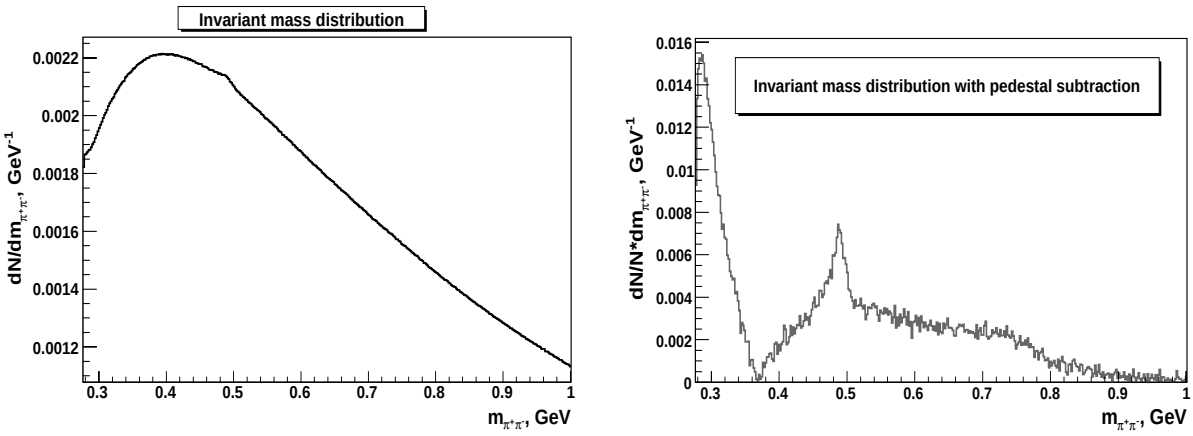

Fig. 1: Invariant mass distribution (a), with subtracted combinatorial background (b)

As it is seen, the significant part of a physical background is cleaned by subtraction of a combinatorial pedestal, so S/B ratio is uncreased within the peak interval.

However, this approach supposes adequate knowledge about particles, which are alternative to the particle of interest in studied events. Since it is not always the case, physicists

have often to guess what kind of processes contribute to form the background. Such an arbitrariness leads often to a stray background (as it seen in fig.1b) and worsen the accuracy of the peak position estimation. Therefore a method is needed that would be able to analyze signals of invariant mass spectra independently of their origin, i.e. of processes generating peaks and background.

Such an approach alternative to above mentioned common methods was proposed in [1]. It is based on the wavelet analysis [2]. Wavelets have particular advantages, which allows to skip the phase of background estimating and to make statistically proved assertion of the peak existing. Besides, wavelets are robust, i.e. resistant to noise. These advantageous properties of wavelets allow to recognize even very small resonance peaks in invariant mass spectra on the huge pedestal of background particles.

After a short introduction to wavelets procedures for peak detection on the basis of discrete and continuous wavelets are described in this paper. Then results of testing the proposed procedures to handle experimental data for K_S^0 mesons produced in d-Au collisions at 200 GeV are given.

2 Brief survey of wavelets

One-dimensional wavelet transform (WT) of the signal f(x) has 2D form. That allows WT to overcome the main shortcomings of the Fourier transform such as: non-locality and infinite support, necessity in a broad band of frequencies to decompose even a short signal.

Wavelet transformation changes the decomposition basis, with functions which are compact into time/space and frequency domain, so WT with wavelet function ψ of function $f(x)$ is defined as

$$W_\psi(a,b)f = \frac{1}{\sqrt{C_\psi}} \int\limits_{-\infty}^{\infty} \frac{1}{\sqrt{|a|}} \psi\left(\frac{b-x}{a}\right) f(x)\, dx \tag{1}$$

with normalization constant

$$C_\psi = 2\pi \int\limits_{-\infty}^{\infty} \frac{|\tilde{\psi}(\omega)|^2}{|\omega|}\, d\omega \;<\; \infty,$$

where $\tilde{\psi}(\omega)$ is Fourier transform of the wavelet $\psi(x)$. The inverse transform is given by formula

$$f(t) = C_\psi^{-1} \int\int \psi\left(\frac{t-b}{a}\right) W_\psi(a,b) \frac{dadb}{a^2} \tag{2}$$

The condition $C_\psi < \infty$ is, at the same time, the condition of the wavelet ψ existence. It holds, in particular, when the first $n-1$ momenta are equal to zero:

$$\int\limits_{-\infty}^{\infty} |x|^m \psi(x) dx = 0, \quad 0 \le m < n. \tag{3}$$

Due to freedom in the choice of the wavelet function ψ many different wavelets were invented [2, 3], but we use in this paper two types of them: some of discrete wavelets

and also continuous wavelets with vanishing momenta, one of which families is named Gaussian wavelets(GW) because they are normalized derivatives of the well known Gauss function

$$g(x; A, x_0) = A \exp\left(-\frac{(x - x_0)^2}{2\sigma^2}\right). \tag{4}$$

Wavelet analysis is accomplished usually by the following steps:

- make a proper choice of a wavelet type
- fulfill a wavelet filtering for de-noising, removing pedestals, and extracting some of needed features of analyzed data.

In its turn the filtering is carried out by:

- transforming data to a wavelet domain
- applying desirable cuts on wavelet 2D-spectrum
- making an inverse transform

2.1 Continuous wavelets with vanishing momenta

The family of continuous wavelets with **vanishing momenta** (VMW) is presented here by Gaussian wavelets, which are generated by derivatives of Gaussian function (4). For canonical Gaussian with $x_0 = 0; \sigma = 1$ one obtains:

$$g_n(x) = (-1)^{n+1} \frac{d^n}{dx^n} \mathrm{e}^{-x^2/2}, \;\; n > 0 \tag{5}$$

The VMW family is called so because the condition (3) is always holds for it.

The normalizing coefficients of these wavelets C_{g_n} are $2\pi(n-1)!$.

It is a remarkable fact that the wavelet transformation of a Gaussian (4) looks as the corresponding wavelet. Therefore the general expression for the n-th wavelet coefficient has the following form (see derivations in [3]):

$$W_{g_n}(a, b)g = \frac{A\sigma a^{n+1/2}}{\sqrt{(n-1)!}s^{n+1}} g_n\left(\frac{b - x_0}{s}\right), \tag{6}$$

where we denote $s = \sqrt{a^2 + \sigma^2}$.

Therefore at the central point $x = x_0$ coefficients of two first even, symmetrical wavelets $W_{G_2}(a, x_0)g$ and $W_{G_4}(a, x_0)g$ obtain their maximum (absolute) values

$$W_{G_2}(a, x_0)g = \frac{A\sigma a^{5/2}}{s^3}, \quad W_{G_4}(a, x_0)g = -\sqrt{\frac{3}{2}} \frac{A\sigma a^{9/2}}{s^5}. \tag{7}$$

One of the attractive features of the wavelet based estimations is their remarkable robustness to background noise, binning range and data missing (see [3]).

2.2 Discrete wavelet transform

Continuous wavelets such as GW gives us a good instrument for the time-frequency analysis of the signal of any possible kind, but they have some shortcomings. Parameters a and b in formula (1) are changing continuously, what leads to the redundant representation of the data. In some cases above mentioned GW properties are quite positive, in particular this redundant representation facilitates the careful spectrum manipulations. The price of this redundancy consists in slow speed of calculations. Besides, GW are nonorthogonal, which disturbs amplitudes of filtered signal after their inverse transform. Moreover, all signals to be analyzed have in practice a discrete structure. Therefore discrete wavelet transforms (DWT) look more preferable for many applications of computing calculations with real data.

To start with a discretization we have to present the scale and shift parameters in the form $a = a_0^m, \quad b = na_0^m; \quad m, n \in Z$ That is, intuitively, clear: with increasing the scale, we should increase a step of shifting too.

The discrete wavelet transform is built by the multi-resolution analysis (MRA), invented by the S. Mallat [4]. The basic idea of the MRA is to represent given signal as its decomposition by two basis functions $\phi_{m,n}(x) = 2^{-m/2}\phi(2^{-m}x - n)$ and $\phi_{0,0} = 2\sum_n h_n\phi(2x - n)$, which must be orthogonal and compact in time/space and frequency domains.

Thus for digital signals the DWT conception is as follows: the original data set, i.e. the sample $\{x_i\}, i = 1..n$ is approximated by a new set $\{\{s_n\}, \{\{d_{j,n}\}\}\}$ of coefficients, which give the wavelet decomposition of the signal. Most remarkable is the number of the coefficients, which we obtained, is equal to the sample size, in contrast to continuous wavelet transform (CWT). The coefficients $s_(j, n)$ — are called approximation, and $d_{j,n}$ — details, which correspond to the decomposition level j. Finally, the decomposition by the DWT of the function $f(x)$ looks like:

$$f(x_i) = \sum_{k=1}^{\frac{N}{2^L}} s_k\phi_{L,k}(x_i) + \sum_{j=1}^{L}\sum_{k=1}^{\frac{N}{2^j}} d_{jk}\psi_{j,k}(x_i) \tag{8}$$

In each decomposition step, the smoothed version of the signal is decomposed to the new more smoothed one and details. Each of the arrays has the half length of the signal. By iterating this procedure we've got the such kind of the decomposition (8).

3 Peak detection using discrete wavelets

To implement peak finding procedure using discrete wavelets we suggest a modification of well-known shinkage procedure (i.e., nonlinear soft thresholding) [6] (see also a survey in [7]), which we called "the adaptive wavelet shrinkage". The term "adaptive" means here that we allow the shrinkage parameter λ in the shrinkage rule [7], to be not a constant, but to depend on the root mean square (RMS) of the wavelet decomposition coefficients on the given decomposition level. We use the linear dependence $\lambda = k * \dot{R}MS$ with parameter k equal to 3, assuming that wavelet coefficients are normally distributed. This choice $k = 3$ should guarantee that we will eliminate the most of the noise components of the signal. Thus, the adaptive shrinkage rule is

$$W_\psi = 0, if|W_\psi| < \lambda, \lambda = k * RMS_i, k = 3, i = scale0, .., scale1$$

We use two different types of discrete wavelets: orthogonal and bi-orthogonal ones with different decomposition bases. After some attempts we chose three families of DWT: Coiflets with one vanishing momentum from the most symmetric wavelet family, Daubechie wavelets with two vanishing momenta and bi-orthogonal CDF44 wavelets [8]. We compare their efficiency applying to the the same example, which was presented above in fig.1(a-b). In fig. $1-2$ there are presented the normalized event distribution

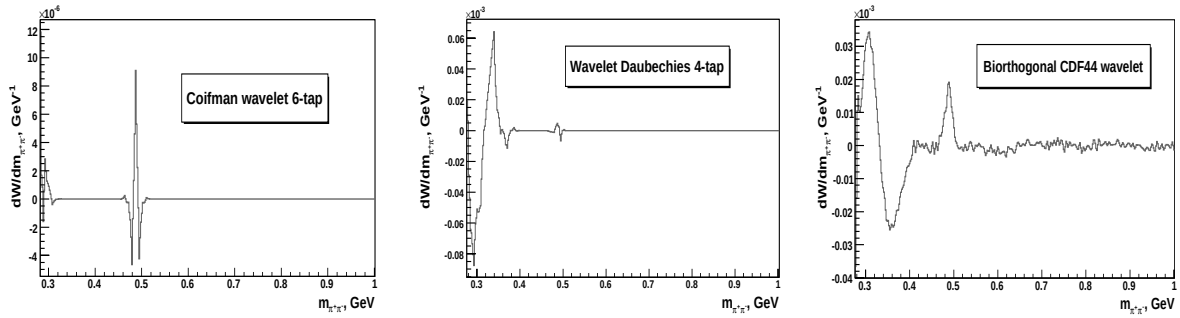

Fig. 2: Wavelet filtering of invariant mass distribution: (a) - Coifman wavelet 6-tap, (b) - Daubechies wavelet 4-tap, (c) - Cohen-Daubechies-Feauveau wavelet (4,4)

$1/N^* \cdot dN/dm_{\pi+\pi^-}$ of invariant weight of the pion pairs produced in central $|\eta| < 0.5$ collisions $d-Au$ at energy 200 GeV in a range $m_{\pi^+\pi^-} = 0.3-1$ GeV.

Fig.2 demonstrates the results of wavelet analysis of the distributions for different discrete wavelets [2, 5]. Wavelet coefficient distribution $dW/dm_{\pi^+\pi^-}$ of pair $\pi^+\pi^-$ invariant mass for Coifman wavelet is shown in fig. $2a$. There are two areas of "irregular" behavior of the distribution: the first relates to the edge effect, the second relates to the existence of resonance peak in the kaon invariant mass interval, which is clearly seen. The peak shape reflects the symmetrical shape of Coifman wavelet function having one maximum and two minima.

The result of applying Daubechies wavelet with two vanishing momenta or 4-tap filter is presented in fig.$2b$. One can see, the strong edge effect on the left, and a small asymmetrical peak in the kaon mass interval. The fig.$2c$ is obtained by applying the bi-orthogonal CDF44 wavelet for the shrinkage procedure. Unlike $2a$ and $2b$ cases where orthogonal wavelets were used, here the influence of background noise component still remains, but the pedestal is completely eliminated, comparing to fig. $1b$. The presence of the resonance peak in the expected region of kaon invariant mass is also clearly indicated. All peaks in fig. $2a, 2b, 2c$ were developed in the wavelet domain at the wavelet scale equal to three, what gave us a rough estimate of the peak width.

The problem of the better precision of the peak position estimation is discussed in the next section.

4 Evaluating peak position by continuous wavelets

In cases when a peak in question has a bell-shape form which could be approximated by a gaussian (4) continuous wavelets can appear to be more suitable to evaluate peak parameters because of the very simple analytical expressions (6) of the gaussian wavelet transform for Gaussian peaks. That allows us to work directly in the wavelet domain instead of time/space domain. Moreover, in real cases when our signal shape is close to a

gaussian and it is considerably contaminated by additive noise and, besides, distorted by binning to be input to computer, one can also use the remarkable robustness of gaussian wavelet filtering proven in [3].

The main idea of our innovative algorithm is to transform the signal to the space of the chosen wavelet (say, G_2 or G_4) domain where the easy analytical formula of the corresponding wavelet surface is valid for our gaussian-like signal. Therefore one can fit this ideal surface to the surface obtained for the real spectrum. To initiate such 2D nonlinear fit one needs a starting point in 2D (a, b) domain, one can find maxima of the wavelet as the solution of equations obtained by differentiating and zeroing each of (7). In this way one would obtain just the 2D maximum of the corresponding wavelet. Although the maximum of a real contaminated signal is inevitably blurred over some area in the wavelet space due to various distortions, it nevertheless, can be used as a good starting point for iterations minimizing a fitting functional.

To realize this idea we tested both G_2 and G_4 gaussian wavelets to filter bell-shaped and distorted signals. Since the study accomplished in [1] for both wavelets shown better performance for G_4, we describe here corresponding considerations and results for this type of wavelets.

We apply G_4 because this wavelets have four vanishing momenta and, therefore, the filtering with them erases any pedestal, if it looks as a parabola. According to (7) one can obtain the maximum of G_4 for a Gaussian (4) in the shift point $b = x_0$ as

$$max_b W_{G_4}(a, x_0)g = -\sqrt{\frac{3}{2}}\frac{A\sigma a^{9/2}}{(a^2+\sigma^2)^{5/2}}. \tag{9}$$

This dependence looks in the wavelet domain of G_4 like a simple curve with one maximum. To find it one has to solve the equation

$$\frac{d(max_b W_{G_4}(a, x_0)g)}{da} = 0.$$

Its solution at the scale a is $a_{max} = 3\sigma$.

In order to test G_4 based filtering we prepare the simulated spectrum of invariant mass, which consists of small gaussian peak at the point $0.47GeV$ and a pedestal produced by a polynomial of the power four.

Result of the filtering such the signal with this scale $a_{max} = 3\sigma$ is shown in fig.3. Although it is hard to recognize peak existence by eyes in fig. $3a$, the corresponding peak is clearly seen in fig. $3b$, where a surface of wavelet coefficients of simulated signal is depicted.

As one can see, the gaussian component of the signal has a form of 2D peak at $0.47GeV$.

It is necessary to point out that the wavelet transformation in this particular example was calculated assuming the signal can be prolonged, if it is needed to avoid edge effects, outside of the boundaries of distribution interval.

Boundaries and pedestal problems. The case of infinite interval is rather artificial, and in practice physicists deal with histograms on the finite interval, which is also splitted into a fixed number of bins. In this case for non-zero pedestal we obtain in the wavelet domain not a single point, as before, but two straight lines restricting an admissible triangle area between two scales:

$$scale_{min} = \frac{7(b_1 - b_0)}{6N_b}, scale_{max} = \frac{(b_1 - b_0)}{6}$$

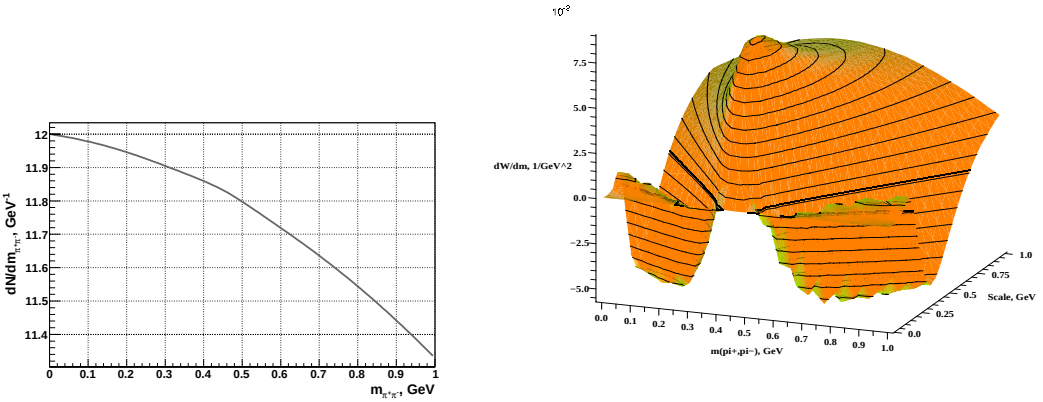

Fig. 3: (a) Invariant mass distribution (signal + background). The resonance is pointed by arrow. (b) Wavelet distribution dW/dm of invariant mass $m_{\pi^+\pi^-}$ for different scales. Results are obtained for infinite interval on $m_{\pi^+\pi^-}$

The minimal scale comes from the constraint of the histogram bin size. The maximal scale is caused by the influence of the boundaries of the finite spectrum interval. So for the real data with finite bounds we have the following constraints defining the fit area: it should be inside of the triangle, which is depicted in fig.4. One can see in fig.5 that outside of this triangle area the edge effects become too strong.

This force us to modify the algorithm of the peak parameter estimation in the way to use only triangle area for fitting in the wavelet domain.

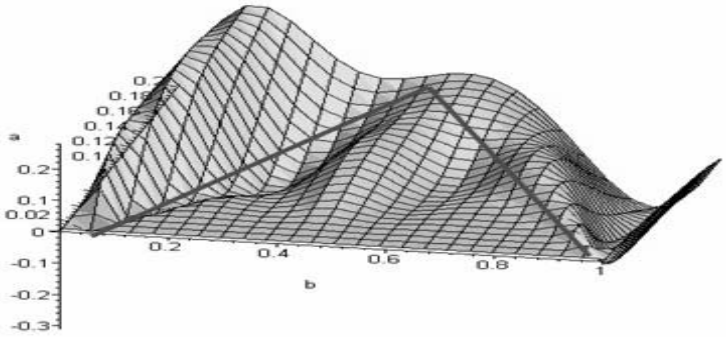

Fig. 4: Wavelet distribution dW/dm of invariant mass $m_{\pi^+\pi^-}$ for different scales. Results are obtained for finite interval on $m_{\pi^+\pi^-}$

5 Application example for neutral K-short meson

We apply the above developed techniques for searching the resonance peak in the spectrum of invariant mass of pion pairs obtained from experimental data, which is presented in fig.6.

We use $240K$ events of the STAR, RHIC&BNL data for d-Au at 200 GeV. The distributions of invariant mass pion pairs are presented in fig. $5a$ and $5b$. Data are taken by the STAR TPC from invariant weight interval from 0.4 up to 0.7 GeV, and pseudo-rapidity interval from -1 up to $+1$. Invariant mass distribution of pion pairs with different signs of charge is shown in fig.$5a$. The combined mass distribution of pairs with

equal signs of charge, which is background for distribution 6a, is shown in fig.5b. Both distributions are normalized. One can hardly guess that there is a peak at 0.49 GeV in fig.5a, which corresponds to mass of the short neutral kaon.

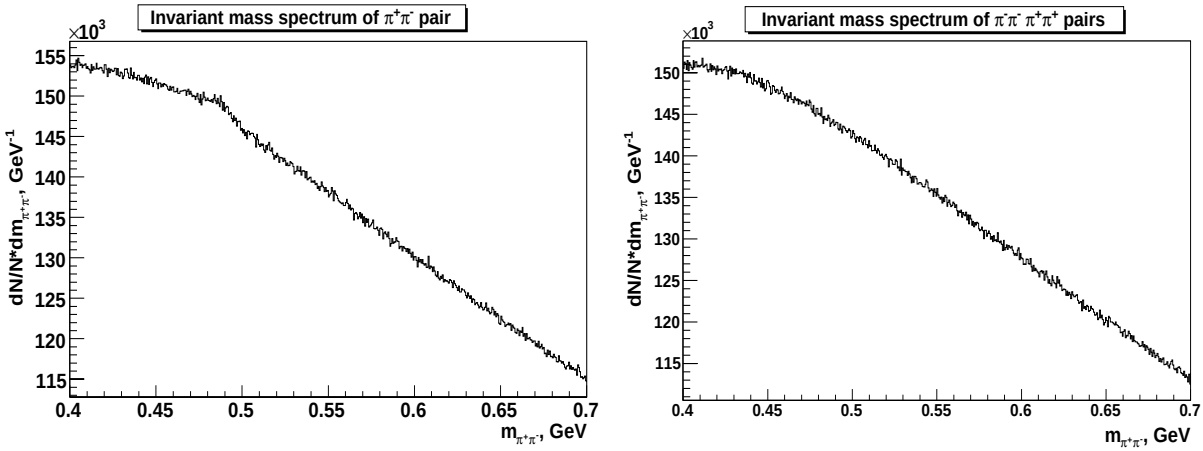

Fig. 5: (a) Normalized invariant mass distribution for $\pi^+\pi^-$ pairs produced in $d-Au$ collisions at $\sqrt{s}$ = 200 GeV. (b) The corresponding combinatorial background. Experimental data are obtained by the STAR collaboration

Then we apply two classical methods of extracting this peak which are based on estimating the pedestal and then subtracting it from the initial spectrum. Results are presented in fig. 6a and 6b. Distribution 6a produced from distribution at the figure 5a by subtraction of the pedestal, which was approximated by a polynomial of the fourth order. Distribution 6b produced from distribution at the figure 5a by subtraction of the pedestal, which was simulated as a combinatorial background and presented in fig.6b. The black thick lines in fig.6a and 6b were obtained as straightforward estimations of Gaussian peaks by χ^2 minimization procedure.

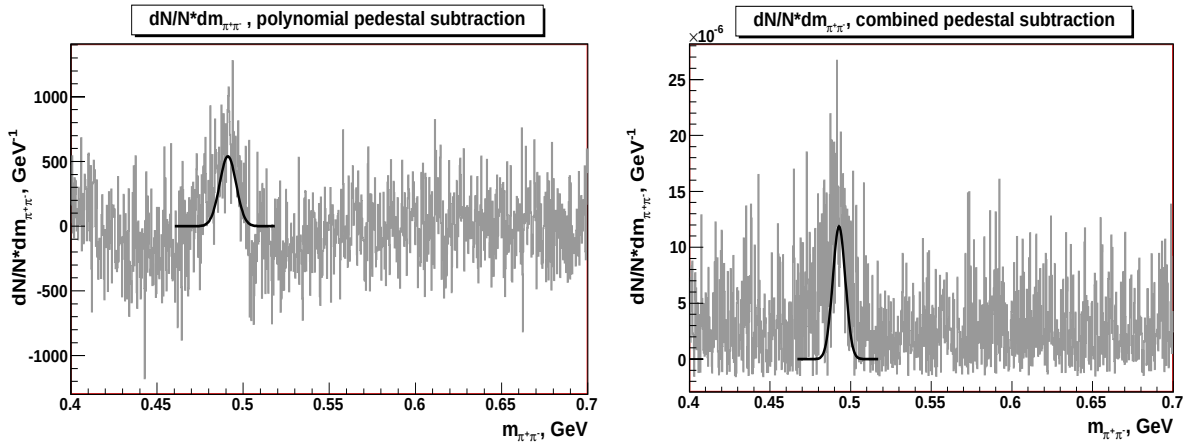

Fig. 6: Normalized invariant mass distribution for $\pi^+\pi^-$ pairs produced in $d-Au$ collisions at $\sqrt{s}$ = 200 GeV with subtracted combinatorial background (a) and polynomial fitted background (b)

The ROOT fitting procedure in wavelet domain inside the triangle area gave us the following results:

- in case of polynomial estimation 0.491095 GeV, in case of combined estimation 0.493544 GeV. Particle Data Group K^0_S invariant mass 0.497648 GeV.

- G_2 gives following results: polynomial estimation 0.488934 GeV, combined estimation 0.505 GeV.
- G_4 gives following results: polynomial estimation 0.487966 GeV, combined estimation 0.498821 GeV.

6 Conclusion

The study made in this paper was caused, from one hand, by the wide popularity of the invariant mass method in contemporary relativistic heavy ion physics and, from another hand, by a dissatisfaction of physicists with carrying out this method which requires a preliminary estimation of combined background, in order to subtract it then from the initial invariant mass distribution.

Since physical processes used to estimate the combined background are not always well-defined, such the background subtraction methods gives sometimes ambiguous and/or inaccurate results.

Therefore a new approach of different nature is proposed here. It is based on the wavelet analysis and allowed to develop algorithms as for resonance peak detecting as for its position estimating.

The new adaptive shrinking algorithm is proposed based on discrete wavelets to detect a peak existence directly without preliminary background estimation and subtraction. Orthogonal and biorthogonal discrete wavelets were compared and eventually the orthogonal coiflet were chosen for adaptive shrinking as the most effective and robust.

Continuous wavelets of gaussian type were studied to evaluate their applicability to estimate resonance peak parameters in presence of bulky complex background. The algorithm applied the G_4 wavelet with special constrains showed its advantage in comparison with conventional methods based on the standard least square fit as well as on the combined background estimation. This comparative study was carried out on the example of searching the K_S^0 invariant mass in the invariant mass spectrum of $\pi^+\pi^-$ obtained on data from the STAR TPC.

References

[1] G.A. Ososkov, A.V. Stadnik and M.V. okarev, Wavelet Approach for Peak Finding in Heavy Ion Physics, JINR Comm. E10-2007-138. Dubna, 2007.

[2] I. Daubechies. The wavelet transform, time frequency localization and signal analysis, IEEE Trans. Inform. Theory 36 (1990), 961-1005.

[3] G. Ososkov, A. Shitov, Gaussian Wavelet Features and Their Applications for Analysis of Discretized Signals, Comp.Phys.Comm, v.126/1-2, (2000) 149-157.

[4] S. Mallat. A theory for multi-resolution signal decomposition: the wavelet representation. IEEE Trans. Pattern Analysis and Machine Intelligence, (1989)

[5] W. Sweldens, I. Daubechies. Factoring Wavelet Transforms into Lifting Steps. Fourier Analysis Applications, vol.4 (1998)

[6] D.L. Donoho and I.M. Johnstone. Ideal spatial adaption via wavelet shrinkage. Biometrika, v.81(1994),425-455.

[7] http://www.toolsmiths.com/docs/CT199809.pdf

[8] I. Daubechies Editor, Proc.of Symp. in Appl. Math.